Anhydrous Proton-Conducting Polymeric Electrolytes for Fuel Cells

S. R. Narayanan,*,† Shiao-Pin Yen,† L. Liu,‡ and S. G. Greenbaum‡

Jet Propulsion Laboratory, California Institute of Technology, Pasadena, California 91109, and Department of Physics, Hunter College of CUNY, New York, New York 10021

Received: July 28, 2005; In Final Form: September 11, 2005

The need to design proton-conducting electrolytes for fuel cells operating at temperatures of 120 °C and above has prompted the investigation of various "water-free" polymeric materials. The present study investigates the properties of "water-free" proton-conducting membranes prepared from high-molecular-weight polymeric organic amine salts. Specifically, the properties of bisulfates and dihydrogenphosphates of poly-2-vinylpyridine (P2VP), poly-4-vinylpyridine (P4VP), and polyvinylimidazoline (PVI) have been investigated over the temperature range of 25−180 °C. Nanocomposites of these polymeric organic amine salts and hydroxylated silica have also been investigated in this study. These polymers are found to be stable and proton-conducting at temperatures up to 200 °C. In all the polymer examples studied herein, the phosphates are more conducting than the bisulfates. The activation energy for ionic conduction was found to decrease with increasing temperature, and this is associated with the increased polymer mobility and ionization of the proton. This is confirmed by the high degree of motional narrowing that is observed in proton NMR experiments. The measured values of conductivity and the differences in pK_a values of the polymeric organic amine and the mineral acid are clearly correlated. This observation provides the basis for the design of other water-free acid−base polymer systems with enhanced proton conductivity. The results presented here suggest that anhydrous polymer systems based on acid−base polymer salts could be combined with short-range proton conductors such as nanoparticulate silica to achieve acceptable conductivity over the entire temperature range.

Introduction

Fuel cells that use a proton-conducting polymer membrane electrolyte have undergone significant development over the past decade. These fuel cells and are now being developed and demonstrated as complete power conversion systems for stationary and transportation applications. The most commonly used polymer membrane electrolyte is the perfluorinated polymer Nafion, a product of DuPont. At ambient pressures of 1 atm and at temperatures below 100 °C, hydrated Nafion has a high proton conductivity of about 0.19 S cm^{-1}.[1] The high proton conductivity of Nafion membranes has allowed that attainment of high power densities and efficiencies.

More recently, it has been recognized that by operating the fuel cell stack at temperatures much higher than 100 °C and even as high as a 180 °C, the overall system size can be reduced and carbon monoxide tolerance can be increased. However, at temperatures above 100 °C, loss of water from the Nafion-type membrane results in a rapid loss of conductivity.[2,3] Several researchers have aimed at modifying Nafion and other materials to retain proton conductivity at temperatures as high as 130 °C and low relative humidity and have been successful to various extents.[4−9] However at 180 °C, few substances can retain water and the realization of an alternate water-based proton conductor presents a significant challenge.

There have been a few successful approaches to realization of proton conductivity at temperatures higher than 130 °C with anhydrous materials. The polybenzimidazole−phosphoric acid membranes extensively researched at Case Western Reserve University[10,11] are now being pursued by developers of stationary fuel cells.[12] Cesium hydrogen sulfate and other inorganic acid salts that undergo a superprotonic phase transition have been investigated by Haile et al.[13,14] Kreuer et al. have shown that imidazole-doped Nafion, where the conduction is carried out by the mobile base constituent, namely, imidazole, does not require water for proton conduction.[15] Takahashi et al. have investigated bisulfates of diethylenediamine and hexamethylenetriamine and found that organic amine salts of protic acids are capable of proton conduction over a wide temperature range.[16] Lassegues et al. have investigated the structure of a variety of polymeric amine salts by infrared spectroscopy and have shown that proton conduction can readily occur through ionization and re-organization of hydrogen-bonded networks.[17] The latter studies were restricted to temperatures below 100 °C.

The present study focuses on measuring the proton-conducting properties of membranes prepared from high-molecular-weight polymeric organic amine salts over a wide temperature range. Specifically, the properties of bisulfates and dihydrogenphosphates of poly-2-vinylpyridine (P2VP), poly-4-vinylpyridine (P4VP), and polyvinylimidazoline (PVI) have been investigated over the temperature range of 25−180 °C. Nanocomposites of these polymeric organic amine salts and hydroxylated silica have also been investigated in this study. The study also focuses on understanding the key factors governing the proton conductivity and the role of acid−base interactions. The materials with the highest values of proton conductivity have been fabricated into membranes and tested as electrolytes in a hydrogen/oxygen fuel cell to demonstrate proton conduction.

* Author to whom correspondence should be addressed. E-mail: s.r.narayanan@jpl.nasa.gov.
† Jet Propulsion Laboratory, California Institute of Technology.
‡ Hunter College of CUNY.

10.1021/jp054167w CCC: $33.50
Published on Web 02/03/2006

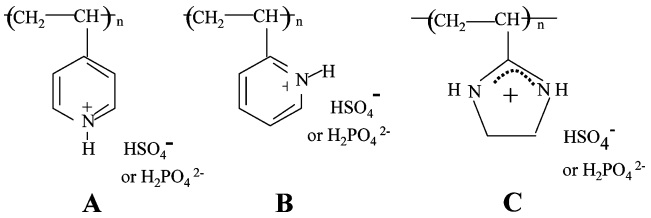

Figure 1. Structures of bisulfates and dihydrogenphosphates of poly-4-vinylpyridine (A, P4VP); poly-2-vinylpyridine (B, P2VP); and polyvinylimidazoline (C, PVI).

Experimental Section

Polymeric Amines and Amine Salts. The chemical structures of materials investigated are shown in Figure 1.

P4VP and P2VP with a molecular weight of 160 000 Daltons were obtained from Scientific Polymers Inc. and used without further purification. Polyvinylimidazoline was synthesized by the cyclization−elimination reaction of polyacrylonitrile with ethylenediamine using thioacetamide as the catalyst.[18] To obtain the quaternized materials, the polymers were at first dissolved in methanol, and this polymer solution was added dropwise into a heated solution of sulfuric or phosphoric acid in methanol. The typical concentration ratio for polymer and acid was one mole of pyridine units in the polymer solution for two moles of acid. Quaternization resulted in precipitation of fine flakes of the polymeric salts that were insoluble in methanol. The salts were filtered and washed with excess methanol several times to remove any traces of excess acid or unreacted polymeric amine. The degree of quaternization was determined using Raman spectroscopy and titration studies. The Raman spectrum for the P4VP and P4VP bisulfate showed the shift of the pyridine quadrant ring stretch from 1600 to 1640 cm^{-1}, indicating complete quaternization. Acid−base titration confirmed the 1:1 composition within experimental error in all cases. Also, the weight gain of the polymer after quaternization was consistent with the ratio of base to acid of 1:1. The 1:1 ratio distinguishes these polymeric salts from other high-temperature electrolyte materials in the literature such as phosphoric acid and polybenzimidazole where the mole ratio of basic nitrogen to acid can be as high as 1:8, with significant amounts of free acid not involved in the quaternization of the polymeric matrix.[19] To prepare a nanocomposite of the polymer salt with silica, a dispersion of nanoparticulate EH-5 (Cabot Corporation) silica was combined with a solution of the polymeric amine in methanol. The latter solution was combined with a solution of the appropriate acid in methanol to precipitate a polymeric amine salt containing nanoparticulate silica. The silica content of these nanocomposite materials was about 10 wt % of the polymeric amine salt.

Preparation of Membranes. Membranes of polymeric amine salts were prepared by solution-casting of concentrated aqueous solutions onto porous supports consisting of nonwoven glass fiber mat (10 g/m^2) or polybenzoxazole mat (26 g/m^2). Solution-cast membranes were allowed to dry in warm flowing air, following which they were dried in a vacuum oven at 60 °C for 2 h. Such processing produced an anhydrous membrane that was flexible and nonporous. The membranes tended to absorb water after prolonged exposure to a moist environment. However, by keeping them in sealed plastic bags, the membrane could be maintained in the dry state.

Thermal Analysis and Ionic Conductivity Measurements. Thermogravimetry (TG) and differential scanning calorimetry (DSC) on the polymer salts was carried out with TA Instruments model 2950/2910. The scan rate for the TG and DSC experiment was 10 °C/min. Prior to these experiments, the samples were dried in a vacuum at 60 °C to remove bulk water. For ionic conductivity measurements, the membranes measuring 6 cm × 6 cm and typically about 0.015-cm thick were assembled in a cell fixture obtained from Electrochem Inc. In this fixture, the membrane sections were held between gold-plated sheets that were held together by graphite blocks. To avoid electronic shorting and overcompression of the membranes, Teflon gaskets were used in the cell. The cell blocks were bolted down to apply a pressure of 200 psi to ensure good interfacial contact. The temperature of the membrane was raised at a fixed rate of 2 °C per minute using the heating elements on the sides of the block. The gold plates that contacted the surfaces of the membrane formed an electrochemically "blocking" interface, as confirmed by impedance measured over a wide range of frequencies using a Solartron 1260 frequency response analyzer. Conductivity as a function of temperature was obtained from impedance at 10 kHz measured with a Agilent 4263B impedance meter. An automated data acquisition system recorded the values during heating and cooling. Each sample was subjected to at least three heating and cooling cycles, and any hysteresis in the curves was noted. Reproducible heating and cooling curves were considered an important indication of stability of the materials. The first heating curve was always ignored because it had features arising from equilibration of the membrane from the cast state. However, after the first heating/cooling cycle, the curves were generally reproducible, and no significant change in the data was observed between the second and fourth cycles. The TG analysis suggested that heating to 180 °C should ensure the removal of any residual bound water in the membranes.

NMR. ^1H ($I = 1/2$) NMR spectra were collected at $B_0 = 7.05$ T (300 MHz) on a Chemagnetics CMX-300 spectrometer. The static ^1H spectra were obtained using a wide-line probe with single-pulse (2-μs pulse width) excitation. Distilled water was used as a frequency reference. Prior to the NMR measurements, the samples (each about 0.5 g) were cut into strips, loaded into open-ended 5-mm OD quartz tubes, and held under roughing vacuum at 60 °C in order to remove residual water. The tubes were then sealed. Temperature control was achieved with ±2 °C accuracy with a standard heated N_2 flow system.

Fuel Cell Studies. Membrane−electrode assemblies were prepared with the most conducting membranes to verify their utility for fuel cells. Catalyst inks were prepared by combining Johnson-Matthey platinum black and poly-2-vinyl pyridinium dihydrogenphosphate. These inks were brush painted on to unteflonized Toray 060 carbon papers to achieve a catalyst loading of 4 mg/cm^2 on both the electrodes. The electrodes with an active area of 25 cm^2 were placed on either side of a membrane and assembled in the cell fixture and raised to 180 °C. The fuel cell experiment was conducted with dry hydrogen and oxygen at flow rates of 0.5 L/min at 1 atm. Polarization measurements were carried out using an in-house fabricated computer-controlled test system. Upon cooling and dis-assembly of the cell, the electrodes were found to have integrally bonded to the membrane.

Results and Discussion

The TG and DSC results on all the samples confirm loss of loosely bound water in the region 70−120 °C. No weight loss or heat absorption/evolution is observed until 200 °C for the phosphates and until 300 °C for the bisulfates. Therefore, in the region of interest for fuel cells, that is, below 200 °C, the materials were determined to be stable. For the phosphates, between 200 and 300 °C a weight loss of about 3−4% is

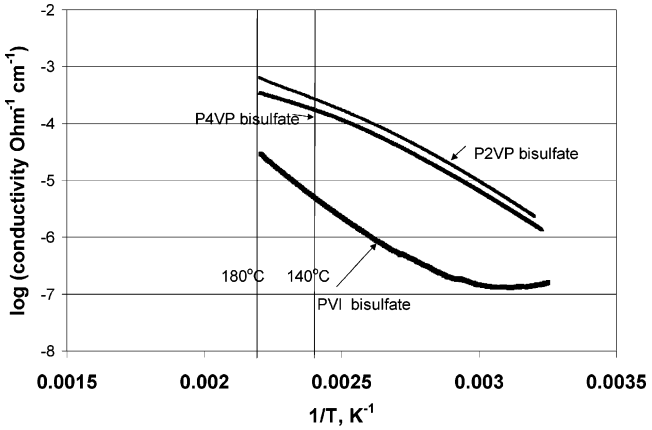

Figure 2. Ionic conductivity of bisulfates of P2VP, P4VP, and PVI as a function of temperature.

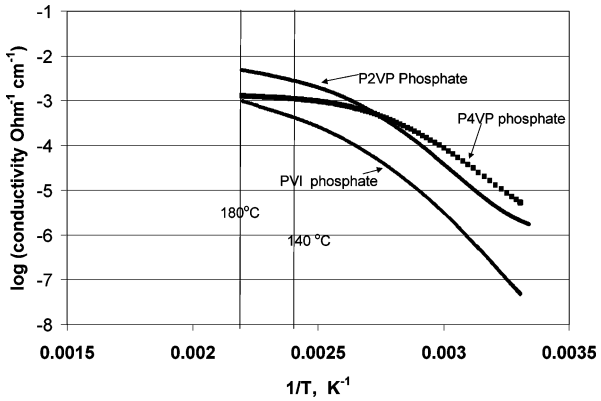

Figure 3. Ionic conductivity of dihydrogenphosphates of P2VP, P4VP, and PVI as a function of temperature.

TABLE 1: Activation Energy Calculated from Conductivity vs 1/*T* Plots for Various Polymer Amine Salts

polymer system	activation energy > 120 °C, eV	activation energy < 120 °C, eV
P2VP bisulfate	0.37 (120−180 °C)	0.57 (30−100 °C)
P4VP bisulfate	0.31 (120−180 °C)	0.55 (30−110 °C)
PVI bisulfate	0.79 (120−180 °C)	not determinable from data
P4VP phosphate	0.03 (160−180 °C)	0.80 (70−30 °C)
P2VP phosphate	0.19 (160−180 °C)	0.92 (70−30 °C)
PVI phosphate	0.34 (130−180 °C)	1.19 (60−35 °C)

observed, attributed to slow release of water by condensation of the dihydrogenphosphate groups to form polyphosphate linkages. Bisulfates do not suffer any significant weight loss until 300 °C. Extensive and continuous weight loss of about 30% observed between 300 and 450 °C with the dihydrogenphosphates and bisulfates is attributed to the decomposition of the organic moieties.

The conductivity of the polymeric bisulfates and dihydrogenphosphates is shown in Figures 2 and 3, respectively. These results indicate that with all the salts studied the conductivity increases with temperature, consistent with thermally activated processes involved in ionic conduction. At temperatures greater than 120 °C, the P2VP salts are found to be more conducting than the P4VP and PVI salts. At 180 °C, the highest conductivity of 0.5×10^{-2} ohm^{-1} cm^{-1} is observed with the P2VP dihydrogenphosphate. Also, in all the polymer examples studied herein, the phosphates are more conducting than the bisulfates.

The activation energy values have been estimated for two ranges of temperature measured from the log{conductivity} vs 1/*T* plots. These values are listed in Table 1. The activation energies at temperatures greater than 120 °C are significantly

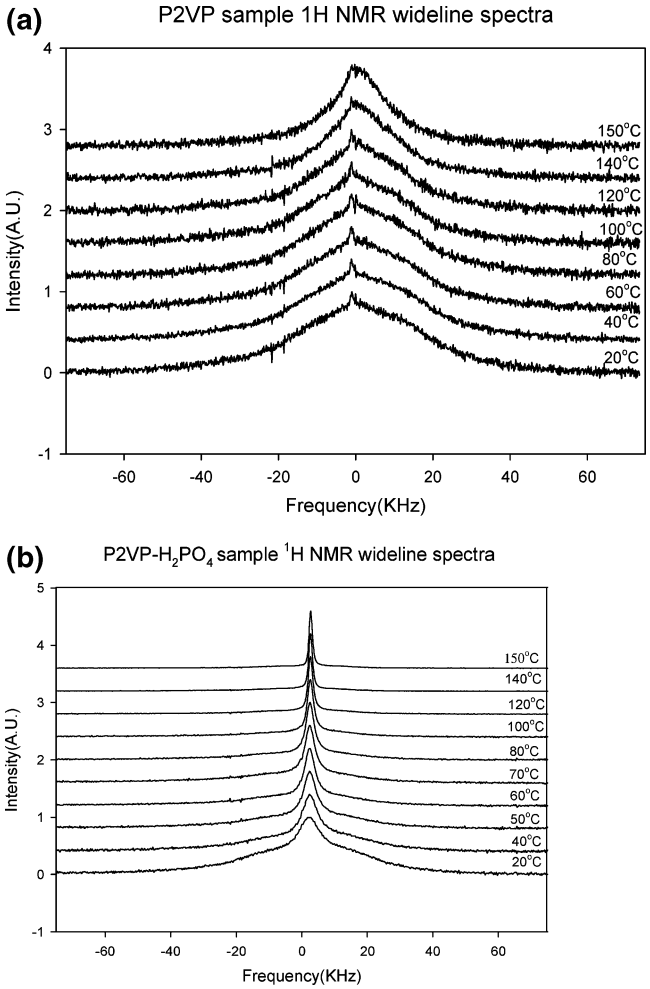

Figure 4. Variable-temperature wide-line proton NMR spectra of P2VP (a) and P2VP−H_2PO_4 (b).

less than the values observed below 120 °C. For the phosphates, the activation energy decreases continuously, without a significant break in the conductivity curve. With the bisulfates the difference between the high- and low-temperature values is not as significant as in the phosphates. Reduction of activation energy with increasing temperature is consistent with increased polymer mobility leading to a higher probability of defect states and higher rates of the reorganization. Proton NMR results confirm that sufficient polymer mobility is present even at 120 °C. Thus, as the temperature is raised well above the T_g of the polymer backbone, a high degree of polymer mobility is achieved, and other factors such as the dissociation equilibria of the proton could become rate-determining. The values of activation energies at high temperatures are similar to those for hydrous oxonium salts and oxides.[17,20]

Figure 4 displays variable temperature ^{1}H NMR spectra for (a) P2VP and (b) P2VP−H_2PO_4. Several features clearly distinguish the quaternized compound from the starting polymer. First, at low temperatures the proton NMR spectrum of P2VP−H_2PO_4 exhibits two components, one of which has a line width comparable to that of the starting compound. Thus, there is convincing evidence for the presence of mobile protons in the phosphate compound, even at relatively low temperature. With increasing temperature the narrower component undergoes further motional averaging, and the broad component becomes relatively less intense and undergoes its own narrowing above ∼100 °C, in contrast to the P2VP material, which shows only very modest motional narrowing over the entire temperature

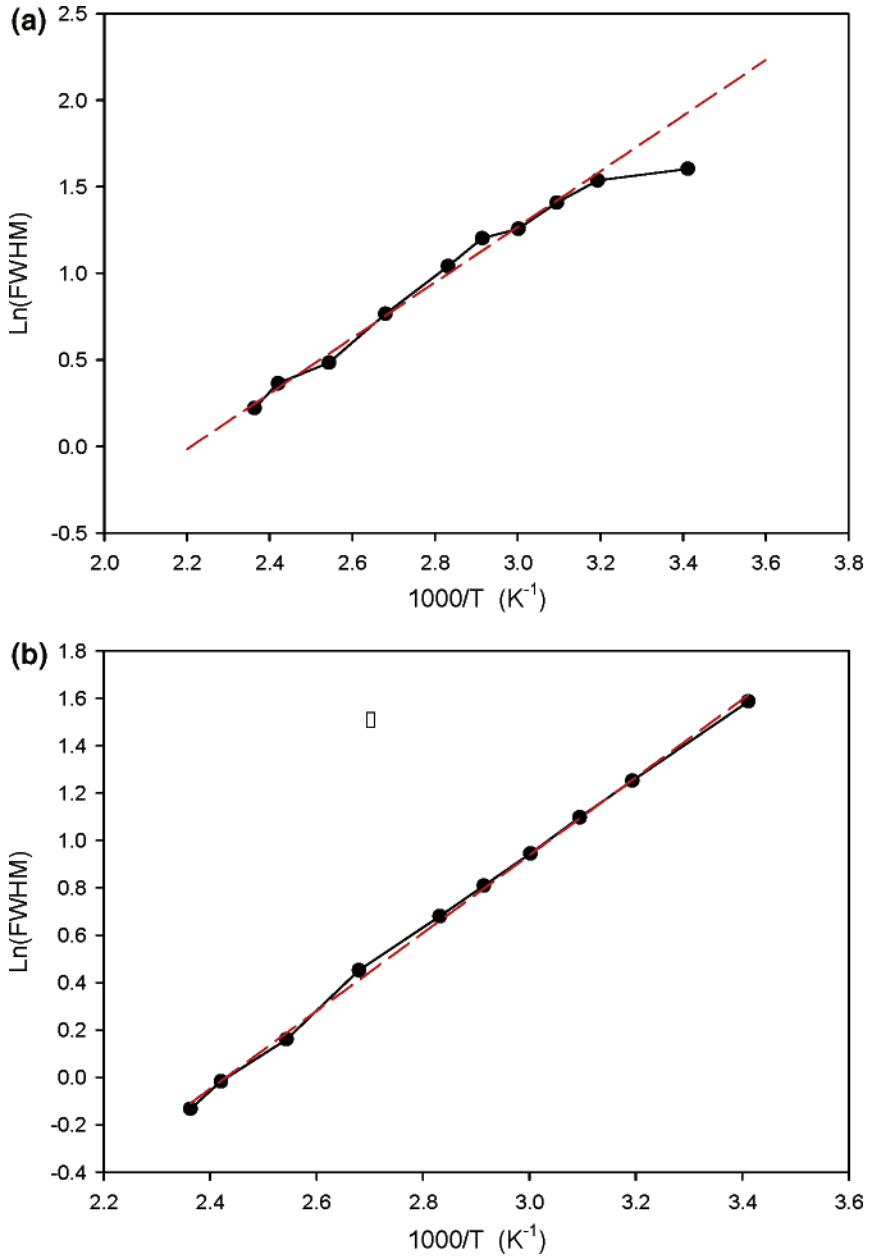

Figure 5. Arrhenius plots of the full width at half-maximum proton NMR line width of P2VP−H_2PO_4 (a) and P4VP−H_2PO_4 (b).

range. A comparison of P4VP and P4VP−H_2PO_4 (not shown) yields a very similar result. Thus, quaternization of the polymer produces mobile protons, as intended, and also apparently facilitates segmental motion within the whole polymer.

The full width at half-height line widths corresponding to the narrow components of P2VP−H_2PO_4 and P4VP−H_2PO_4 are plotted in Figure 5, parts a and b, respectively. Both curves yield an activation energy of about 0.14 eV, which is substantially lower than that given by the conductivity measurements. Disagreements between conductivity and NMR line width activation energies are frequently observed for several reasons, including the different time scales probed by the different techniques. Another possible source of the discrepancy is that NMR activation energies could just reflect polymer mobility and may not capture the ionization of the proton. It is noteworthy that both quaternized compounds yield quite similar behavior, strongly suggesting a common transport/segmental motion mechanism.

The ratio of the conductivity of the corresponding dihydrogenphosphates and the bisulfates of the polymeric organic amines taken at 180 °C is the highest for PVI and is about 31.6, while those for P4VP and P2VP are 3.9 and 7.4, respectively. If the polymer mobility chiefly determined the conductivity, then the ratios would be similar for all the polymeric amines at 180 °C, as all the polymers are highly mobile at this temperature. However, the large variance in this ratio observed between the polymers suggests that when polymeric mobility is achieved, there are other factors that determine the conductivity, as discussed below.

Since proton conductivity is also dependent on proton availability, the acid−base interactions between the polymer amine and the acid anion are likely to play a major role. For such "water-free" polymeric salts, proton transport involves ionization followed by the transfer of the ionized proton through the reorganization of hydrogen bonds as in the "Grotthuss mechanism", and this was suggested by Lassegues et al.[17] Sulfuric acid, phosphoric acid, and the quaternized polymeric amines are significantly different in the proton dissociation tendencies. Thus, differences in conductivity observed at high temperature when the polymer chains are mobile could be

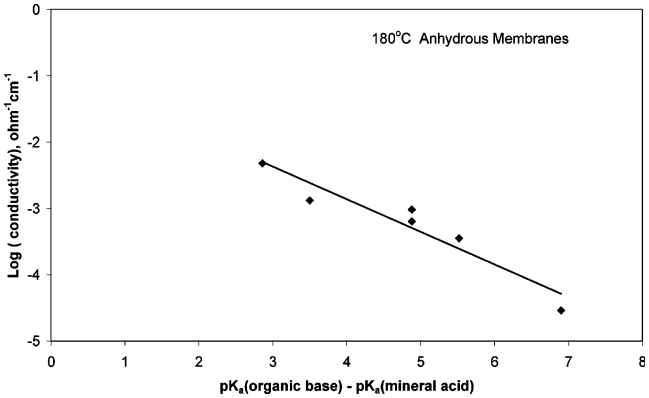

Figure 6. Dependence of conductivity at 180 °C on the difference of p*K* values of polymeric organic amine and base.

attributed to the concentration of protons available for transfer from the acid to base sites. These dissociation properties are reflected in the free-energy change of the acid−base reactions as follows.

The proton dissociation of the polymeric amine salt may be represented as follows:

$$\text{poly NH}^+ + \text{X}^- = \text{poly-N} + \text{HX} \qquad (1)$$

Since ionization provides a proton source, a large degree of ionization of the proton will result in high conductivity. The neutral amine species formed by ionization of the proton gives rise to the defect sites for accepting a proton. Alternately, a lower free-energy change for the above reaction ensures higher concentration of the protonic species and weaker interaction between the ion pair. To calculate the free-energy change of reaction 1 we use aqueous dissociation constants for polymeric amine and acid in aqueous media and combine them using Hess's law as follows:

$$\text{poly NH}^+ + \text{H}_2\text{O} = \text{poly N} + \text{H}_3\text{O}^+ \qquad (2)$$

The standard free-energy change for the process in eq 2 is given by

$$\Delta G^0{}_2 = 2.303RT\,(\text{p}K_{a,\ \text{polyNH+}})$$

$$\text{HX} + \text{H}_2\text{O} = \text{H}_3\text{O}^+ + \text{X}^- \qquad (3)$$

The standard free-energy change for the process in eq 3 is given by

$$\Delta G^0{}_3 = 2.303RT\,(\text{p}K_{a,\ \text{acid}})$$

Therefore, using Hess' law, the free-energy change for reaction 1 is given by

$$\Delta G^0{}_1 = \Delta G^0{}_2 - \Delta G^0{}_3 = 2.303RT\,(\text{p}K_{\text{a,polyNH+}} - \text{p}K_{\text{a,acid}}) \qquad (4)$$

According to eq 4, the free-energy change of reaction 1 is related to the difference in the acid dissociation constant for the polymeric amine and the acid. For the three polymeric amines and two types of acids studied in this work, the free-energy change can be calculated. The dependence of conductivity at 180°C on this free-energy change is now explored. Figure 6 shows a linear dependence of log(conductivity) on the difference in pK_a values of the polymeric amine base and the acid. Thus, with smaller differences in pK_a of the polymeric amine and the acid, higher conductivity values are attained. This correlation extends over three orders of conductivity. The results in Figure 6 confirm that with a combination of acid and base materials with a small difference in pK_a, a high concentration of "free" proton charge carrier can be generated.

TABLE 2: High-Temperature Activation Energy Values from Table 1 Compared with Free-Energy Values Calculated from Eq 4

electrolyte type	activation energy from experiment, eV	activation energy calcd from eq 4, eV
P2VP bisulfate	0.37	0.42
P2VP phosphate	0.19	0.24
P4VP bisulfate	0.31	0.47
P4VP phosphate	0.03	0.36
PVI bisulfate	0.79	0.66
PVI phosphate	0.34	0.39

On the basis of the correlation shown in Figure 6, the conductivity of the acid−base polymer systems can be expressed as follows:

$$\log K = \log K_o - (\text{p}K_{\text{a,organic base}} - \text{p}K_{\text{a,mineral acid}}) \qquad (5)$$

Substituting from eq 4,

$$\log K = \log K_o - (\Delta G^0{}_1/2.303RT) \qquad (6)$$

On the basis of eq 6, $\Delta G^0{}_1$ could now be viewed as the activation energy governing conduction.

In Table 2, the experimentally determined activation energy values at 180 °C are compared with the free-energy change for the acid−base equilibrium of eq 1, calculated using eq 4. The pK_a values used were 5.0 for P2VP, 5.6 for P4VP, and 7.0 for PVI. In most of the cases studied, the observed and calculated values of activation energy are quite close in magnitude. This reasonably close agreement between the calculated and observed activation energies in five of the six cases suggests that, at high temperatures where barriers of polymer mobility are overcome, acid−base interactions and the ionization process govern the value of ionic conductivity. Some of the differences between calculated and observed values could arise from the fact that pK_a values for polymers vary with the degree of ionization. The deviation in the case of P4VP phosphate is not entirely clear at this time, although the lower T_g and melting point of this polymer salt could be factors. Thus, the dependence of conductivity on the acid−base interactions presents a first-order explanation to the differences in conductivity values observed at temperatures of 180 °C.

At lower temperatures where the activation energy values are higher, transport barriers arising from polymer mobility will have additional contributions, and the conductivity cannot be correlated to the acid−base interactions alone. Also, the slow variation of activation energy at lower temperatures (<120 °C) could be similar to the Vogel−Tamman−Fulcher (VTF) behavior commonly observed in amorphous lithium conducting polymer electrolytes which has been described by various groups in terms of free volume or configurational entropy considerations.[21,22]

Effect of Nanoparticulate Silica. Membranes of the polymeric amine salts combined with 10−20% of nanoparticulate silica were fabricated. Conductivity results showing the effect of addition of nanoparticulate silica are shown in Figure 7. Silica reduces the activation energy for conduction below 120 °C and increases the conductivity by over an order of magnitude at these lower temperatures; however, the conductivity at temperatures greater than 120 °C is affected only to a small extent. The

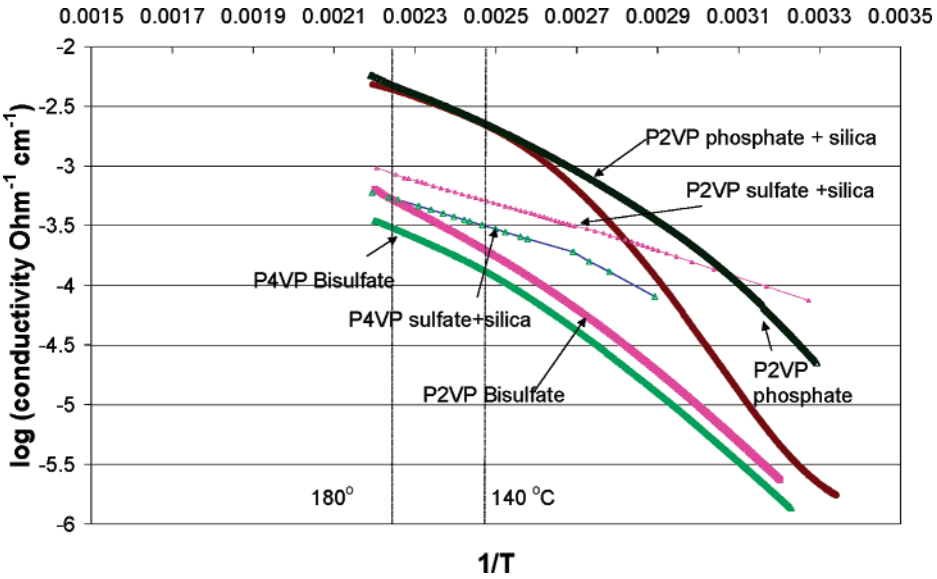

Figure 7. Ionic conductivity of nanocomposites of silica and polymer amine salts.

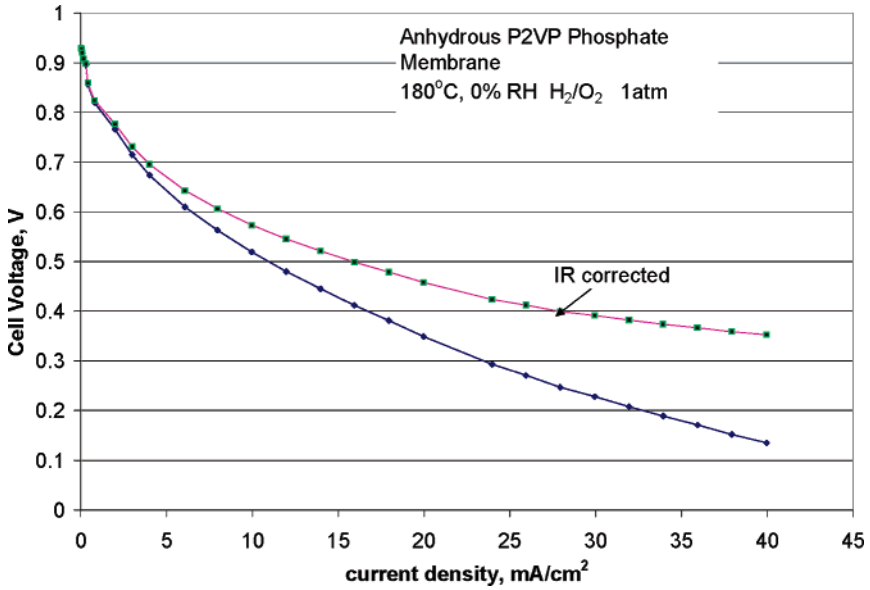

Figure 8. Performance of "water-free" P2VP hydrogenphosphate membrane-based fuel cell, 1 atm hydrogen and oxygen, at 180 °C.

observation that the barrier at low temperature is the one that is affected suggests that effects beyond that described by the VTF model are operating. The 20−30-nm particles of silica in Carb-o-sil EH-5 have a chain-forming tendency resulting in aggregates that can bestow unique properties when blended with liquids and polymers.[23] This particular type of silica has about four proton-conducting −OH groups per square nanometer of the silica surface. This amounts to approximately 50% of the surface being covered with such Si−OH groups. These Si−OH groups interact strongly through hydrogen bonding and can potentially conduct protons when a proton source is available. The thermal stability and chemical inertness of these silica materials is also extremely good. The enhanced conductivity and the reduction in activation energy confirms that the silica can be used to enhance the conduction by providing more hopping sites for conduction of ionized protons.

Fuel Cell Studies. Fuel cells were fabricated from the most conducting of the polymeric electrolytes and operated with hydrogen and oxygen. These experiments demonstrated that the electrolyte materials are hydrogen ion conductors and useable in a fuel cell configuration. The ionic conductivity measurements by themselves do not establish that the observed conductivity arises from protons. The behavior of the membranes in an electrochemical cell is thus an important investigation. The high open-circuit voltage suggested that the electrochemical equilibria observed with conventional proton conductors is also observed with these polymeric salts. The high open-circuit voltage also confirms that fuel crossover through the membrane was not significant, although separate measurements of hydrogen permeability will be needed to confirm this. The results of polarization measurement on a cell fabricated from poly-2-vinylpyridinium phosphate at 180 °C are shown in Figure 8. The current density of about 30 mA/cm^2 at 0.4 V is observed after correction for internal resistance of the electrolyte. The observation of a steady-state current suggests that protons produced at the anode diffuse and migrate across the membrane and react with oxygen at the cathode, confirming that the polymeric salts are functioning as proton conductors. Thus, limitations to power density arising from interfacial processes appear to be more significant than the low conductivity of the electrolyte. These interfaces could be poorly formed given that porous platinum−electrolyte composite electrodes have not been optimized for electrolyte

distribution and electrolyte content. Optimization of membrane electrode assemblies would be an important step in the realization of higher power densities.

Conclusions

The properties of membranes prepared from poly-2-vinylpyridinium, poly-4-vinylpyridinium, and polyvinylimidazolinium salts (1:1) prepared by quaternization with sulfuric and phosphoric acids has been investigated. These polymers are found to be stable and proton-conducting up to 200 °C. In all the polymer electrolyte examples studied herein, the phosphates are more conducting than the bisulfates. The studies suggest that the higher conductivity can be explained by the smaller difference in pK_a values of phosphoric acid and the polymeric amine, as compared to the sulfuric acid and the polymeric amine. Thus, at temperatures where polymer mobility is no longer a big barrier to proton transport, a correlation has been observed between conductivity and the difference in pK_a values of the polymeric organic amine and the mineral acid. The smaller the difference in pK_a values, the higher the observed conductivity value. This correlation provides the basis for the design of other water-free acid−base polymer systems with enhanced proton conductivity. In such a materials design approach, a polymer system with a strong acidic component (low pK_a value) that thermodynamically allows the facile ionization of the proton can be combined with a very weakly basic site that can accept the proton but not bind too strongly to it to provide high proton conductivity. This correlation holds true when the polymer chains are conformational mobile and the defects are regenerated continuously. The activation energy for ionic conduction was found to decrease with increasing temperature, and this is associated with the increased polymer mobility and ionization of the proton. This is confirmed by the high degree of motional narrowing that is observed in proton NMR experiments. The activation energy for conduction at temperatures when the polymer salts are conformationally mobile correlates well with free-energy change in the acid−base interactions. Addition of nanoparticulate increases the conductivity substantially at temperatures where the polymer backbone is not mobile. This suggests that the acid−base properties and the chainlike arrangement of nanoparticulate silica particles can be used to lower the barriers for proton conduction in materials where polymer motion is hindered. The findings reported herein could be extended to polymer acid−polymer base systems and used as a basis for the design of anhydrous polymer systems with two or more components to achieve acceptable conductivity over the entire temperature range.

Acknowledgment. This work was carried out at the Jet Propulsion Laboratory, California Institute of Technology, under a contract with the National Aeronautics and Space Administration. The U.S. Department of Energy, Office of Energy Efficiency and Renewable Energy, High Temperature Membrane Program, funded the effort. The research at Hunter College was supported in part by a grant from the Office of Naval Research and an RCMI Infrastructure grant (RR-03037) from the National Institutes of Health.

References and Notes

(1) Zawodzinski, T. A.; Neeman, M.; Sillerud, L. O.; Gottesfeld, S. *J. Electrochem. Soc.* **1993**, *140*, 1041−1047.

(2) Anantaraman, A. V.; Gardner, C. L. *J. Electroanal. Chem.* **1996**, *414*, 115−120.

(3) Sone, Y.; Ekdunge, P.; Simonsson, D. *J. Electrochem. Soc.* **1996**, *143*, 1254−1259.

(4) Yang, C.; Srinivasan, S.; Bocarsly, A. B.; Tulyani, S.; Benziger, J. B. *J. Membr. Sci.* **2004**, *237*, 145−161.

(5) Malhotra, S.; Datta, R. *J. Electrochem. Soc.* **1997**, *144*, L23−L26.

(6) Miyaki, N.; Wainright, W. S.; Savinell, R. F. *J. Electrochem. Soc.* **2001**, *148*, A898−A904.

(7) Yang, B.; Manthiram, A. *J. Electrochem. Soc.* **2004**, *151*, A2120.

(8) Ramani, V.; Kunz, H. R.; Fenton, J. M. *J. Membr. Sci.* **2004**, *232*, 31.

(9) Kim, Y. S.; Wang, F.; Hickner M.; Zawodzinski, T. A.; McGrath, J. E. *J. Membr. Sci.* **2003**, *212*, 263−282.

(10) Wainright, J. S.; Savinell, R. F.; Litt, M. H. In *Proceedings of the Second International Symposium on New Materials for Fuel Cell and Modern Battery Systems*; Savadogo, O., Roberge, P. R., Eds.; Montréal, Canada, 1997; p 808.

(11) Savadogo, O.; Xing, B. *J. New Mater. Electrochem. Syst.* **2000**, *3*, 345−349.

(12) Staudt, R. Development of Polybenzimidazole-based High-Temperature Membrane and Electrode Assemblies for Stationary and Transportation Applications, 2005 DoE Hydrogen, Fuel Cells and InfraStructure Program Review, presentation available at http://www.eere.energy.gov/hydrogenandfuelcells/pdfs/review05/fc8_staudt.pdf.

(13) Boysen, D. A.; Chisholm, C. R. I.; Haile, S. M.; Narayanan, S. R. *J. Electrochem. Soc.* **2000**, *147*, 3610−3614.

(14) Haile, S. M.; Boysen, D. A.; Chisholm, C. R. I.; Merle, R. B. *Nature* **2001**, *410*, 910−913.

(15) Kreuer, K. D.; Fuchs, A.; Ise, M.; Sapeth, M.; Mater, J. *Electrochim. Acta* **1998**, *43*, 1281−1288.

(16) Takahashi, T.; Tanase, S.; Yamamoto, O.; Yamauchi, S. *J. Solid State Chem.* **1976**, *17*, 353−361.

(17) Lassegues, J. C. In *Protonic Conductors*; Colomban, P., Ed.; Cambridge University Press: Cambridge, 1992; p 311. (b) Trinquet, O. Thesis, University of Bordeaux, 1990.

(18) Drennen, T. H.; Kelley, L. E. U.S. Patent 3,376,159, 1968.

(19) Ma, Y.-L.; Wainright, J. S.; Litt, M. H.; Savinell, R. F. *J. Electrochem. Soc.* **2004**, *151*, A8−A16, and references therein.

(20) Colomban, P.; Novak, A. In *Proton Conductors*; Colomban, P., Ed.; Cambridge University Press: Cambridge, 1992; p 273.

(21) Schuster, M. F. H.; Meyer, W. H.; Schuster, M.; Kreuer, K. D. *Chem. Mater.* **2004**, *16*, 329−337.

(22) Bendler, T.; Fontanella, J. J.; Shlesinger, M. F.; Wintersgill, M. C. *Electrochim. Acta* **2003**, *48*, 2267−2272 and references therein.

(23) Data sheet on Carb-o-sil EH-5 provided by Cabot Corporation, available at http://w1.cabot-corp.com under fumed metal oxide products.